Error Control Coding and Space-Time MMSE Multiuser Detection in DS-CDMA Systems

Walaa Hamouda and Peter J. McLane

Abstract: **We consider the use of error control coding in direct sequence-code-division multiple access (DS-CDMA) systems that employ multiuser detection (MUD) and space diversity. The relative performance gain between Reed-Solomon (RS) code and convolutional code (CC) is well known in [1] for the single user, additive white Gaussian noise (AWGN) channel. In this case, RS codes outperform CC's at high signal-to-noise ratios. We find that this is not the case for the multiuser interference channel mentioned above. For useful error rates, we find that soft-decision CC's to be uniformly better than RS codes when used with DS-CDMA modulation in multiuser space-time channels. In our development, we use the Gaussian approximation on the interference to determine performance error bounds for systems with low number of users. Then, we check their accuracy in error rate estimation via system's simulation. These performance bounds will in turn allow us to consider a large number of users where we can estimate the gain in user-capacity due to channel coding. Lastly, the use of turbo codes is considered where it is shown that they offer a coding gain of 2.5 dB relative to soft-decision CC.**

Index Terms: **Code division multiple access (CDMA), space-time filtering, multiuser detection, Reed-Solomon codes, convolutional codes, turbo codes, performance analysis.**

I. INTRODUCTION

The use of adaptive antenna arrays in mobile radio systems to combat cochannel interference was first introduced in the early 1980's [2]. Moreover, the capability of an adaptive antenna array to discriminate between signals arriving at different angular distributions made it suitable for multiple access techniques to increase the system capacity and improve its performance. In the literature, a considerable amount of work has been conducted on combining antenna array processing with uncoded MUD (e.g., [3] and [4]). In [3], Miller and Schwartz have introduced the optimum space-time maximum likelihood sequence estimator (MLSE). It has been shown in [3], that such an optimum detector consists of a bank of beamformers followed by the joint ML sequence estimator. In the same article, the suboptimum linear space-time MUD's were analyzed and compared to their temporal counterpart.

In DS-CDMA, there has been little work conducted on employing error control coding in systems with space-time MUD. Most of the literature on channel coding in CDMA systems has been only focused on the second generation (2G) matched filter receiver [5]–[8] and not on space-time MUD. Other works on space-time MUD and channel coding include the work by Pickholtz *et al.* [9] where they have considered the use of space-time MUD in conjunction with error control coding. In their work, the optimum space-time MLSE for a synchronous DS-CDMA system with rate $1/n$ convolutional code was derived for the AWGN channel. In [10], Reed and Alexander have proposed an iterative multiuser detection algorithm using channel coding and antenna arrays. Also, Giallorenzi and Wilson in [11] have proposed suboptimum joint multiuser detection and decoding approaches using convolutional codes in asynchronous DS-CDMA systems. Recently, Wong and Lataief [8] have investigated the use of serial concatenated coding in DS-CDMA systems over frequency-selective Rayleigh fading channels, however space-time detection was not considered in their treatment.

In this paper, we develop an in-depth study of DS-CDMA systems that employ error control coding and space-time MUD. We consider three important coding techniques; RS, CC, and turbo coding. Our contribution is to determine how much error control coding can improve the performance of DS-CDMA systems with space-time MUD. We focus on both AWGN and Rayleigh fading channels. We first obtain error bounds for the coded systems. Then, for a small number of users, we examine the accuracy of these bounds when compared to exact system's performance. Finally, with the aid of error bounds, we perform a user-capacity investigation where we assess the capacity improvement relative to an uncoded system with the same diversity order.

In [1], RS and CC are compared for a single user AWGN channel. It is shown that, RS codes can outperform CC at error rates around one part in 10 million. On the other hand, in the interference channel, we find that convolutional codes offer a better performance than RS codes at all feasible error probabilities. For instance, in a perfectly interleaved Rayleigh fading channel with perfect channel state information at the receiver, we find that CC offers a capacity improvement of 250% relative to a system with no error control coding. In a realistic channel model, both channel estimation and interleaving will not be ideal, and hence, deviations from ideal capacity gains are possible. However, we find that there is a synergy at work with the use of coding in space-time systems. In this case the antenna array strongly attenuates interference arriving outside its beamwidth and for those users within the array beamwidth, multiuser detection plus coding serve to return the performance to acceptable norms.

The paper is organized as follows. In Section II, the system model for the space-time MMSE-MUD with channel coding is presented. In Section III, the space-time MMSE-MUD is introduced for both the AWGN and the flat Rayleigh fading channels. Section IV presents both analytical and simulation results for the

Manuscript received February 13, 2003; approved for publication by Marco Lops, Division I Editor, July 14, 2003.

W. Hamouda is with the Department of Electrical and Computer Engineering, Concordia University, Montreal, Quebec, Canada, email: hamouda@ece.concordia.ca.

P. McLane is with the Department of Electrical and Computer Engineering, Queen's University, Kingston, Ontario, Canada, email: mclane@ee.queensu.ca.

1229-2370/03/$10.00

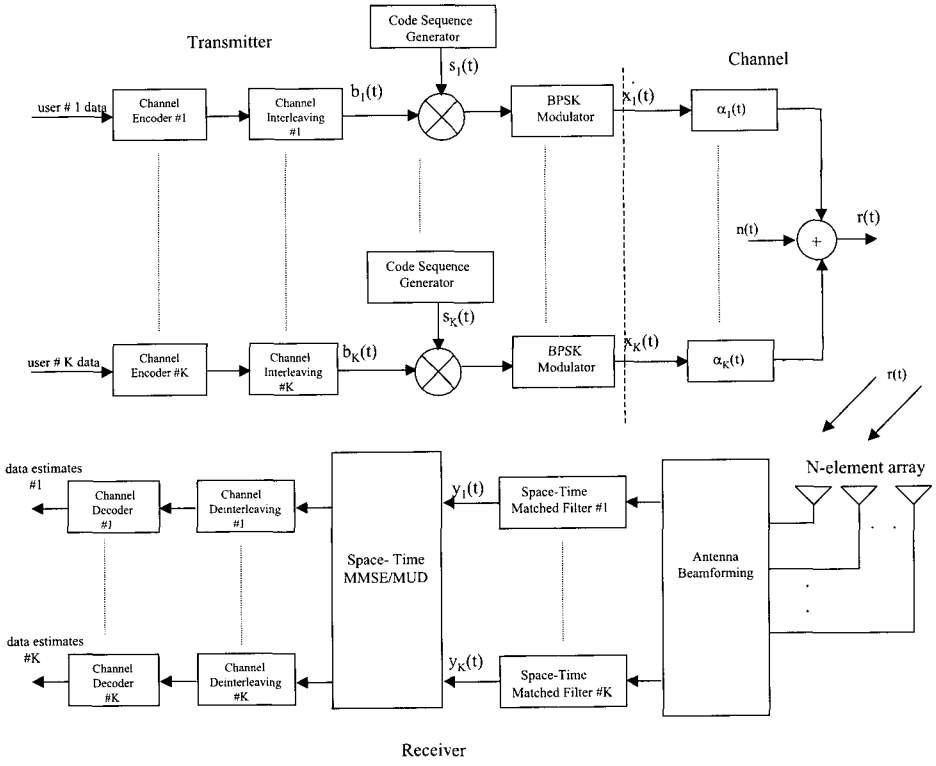

Fig. 1. Space-time MMSE-MUD coded system.

coded system in AWGN channels. In Section V, the probability of bit error for the MMSE-MUD over frequency-flat Rayleigh fading channels is derived and then used to obtain error bounds for the coded system. Simulation results and theoretical performances are compared in Section V along with several important system issues. Finally, conclusions are given in Section VI.

II. CODED DS-CDMA SYSTEM MODEL

The system under study is schematically shown in Fig. 1. As shown, each user's signal of m information bits is first encoded using a rate $R = m/n$ channel encoder to produce n coded symbols. After channel interleaving, these coded symbols are spread using a unique code sequence known only to the receiver base-station. Finally, modulation takes place and users transmit their signals over the radio channel. These signals are superimposed on each other forming a multiuser signal that is corrupted by the channel (i.e., AWGN and flat fading). At the front-end of the receiver, an N-element array is used followed by a bank of space-time matched filters to form the sufficient statistics for users' data detection. The outputs of these space-time matched filters are then applied to the MMSE-MUD for interference cancellation, and then finally, to a bank of deinterleavers followed by channel decoding. In our analysis, we first consider a fully interleaved fading channel and then we study the effects of practical channel interleaving on our results.

Considering a complex channel model, the received multiuser signal in baseband form can be simply written for a K-user system as[1]

$$\mathbf{r}(t) = \sum_{k=1}^{K} \sqrt{E_k}\alpha_k(t)s_k(t)\ b_k(t)\mathbf{u}_k + \mathbf{n}(t), \qquad (1)$$

where for any user k, E_k is the received signal energy per coded bit, related to the uncoded signal energy through $E_k = RE_b$, where $R = m/n$ is the code rate and E_b is the energy per information bit, $s_k(t)$ is the complex signature waveform, $b_k(t) \in \{1, -1\}$ is the coded information sequence, $\alpha_k(t) = |\alpha_k(t)|e^{i\phi_k(t)}$ is the complex channel gain which is assumed to be constant over one symbol interval, $\mathbf{n}(t)$ is the complex Gaussian noise vector with real and imaginary components independent normal Gaussian random processes with variance $\sigma^2 = N_o/2$ per dimension. Note that the complex array response vector in (1) is given by

$$\mathbf{u}_k = \left[\ 1\ \ e^{-j(n-1)\pi \sin\theta_{k,2}}\ \ \cdots\ \ e^{-j(n-1)\pi \sin\theta_{k,N}}\ \right]^T, \qquad (2)$$

where T represents matrix transpose, and $\theta_{k,n}$ is the angle-of-arrival (AOA) of the kth user signal at the nth array element. Using (1), the sampled output of the kth space-time matched filter can be written as

$$y_k = \hat{\mathbf{u}}_k^H \sqrt{E_k}\ \alpha_k b_k \mathbf{u}_k + \hat{\mathbf{u}}_k^H \sum_{j\neq k}^{K} \sqrt{E_j}\ \alpha_j b_j \rho_{kj}\mathbf{u}_j + \gamma_k, \qquad (3)$$

[1] In the paper, vectors will be referred to by bold letters, while scalar quantities will be referred to by italic letters.

where

$$\rho_{kj} = \int_0^{T_s} s_k^*(t) s_j(t) dt, \tag{4}$$

is the cross-correlation factor between the kth and the jth users, and γ_k is a complex Gaussian noise given by

$$\gamma_k = \hat{\mathbf{u}}_k^H \int_0^{T_s} \mathbf{n}(t) s_k^*(t) dt, \tag{5}$$

where T_s is the symbol interval and the superscript H signifies Hermitian transpose. In (3), $\hat{\mathbf{u}}_k$ is the steering vector estimate for user k and in this paper we take $\hat{\mathbf{u}}_k = \mathbf{u}_k$.

III. SPACE-TIME MMSE DETECTION

From (3), the output of the matched filter bank can be written in a vector form as

$$\mathbf{Y} = \mathbf{G}\boldsymbol{\alpha}\sqrt{\mathbf{E}}\mathbf{b} + \mathbf{N}, \tag{6}$$

where the matrices $\boldsymbol{\alpha}$,$\mathbf{Y}$, $\mathbf{G}$, $\mathbf{N}$, and $\sqrt{\mathbf{E}}$ are omitted here but defined in the Appendix. Now, the space-time MMSE-MUD receiver can be defined for the AWGN channel by [12]

$$\mathbf{T}_{MMSE} = \left(\mathbf{G} + \sigma^2 \mathbf{E}^{-1}\right)^{-1}, \tag{7}$$

and for the Rayleigh fading channel by [13]

$$\mathbf{T}_{MMSE} = \left[\mathbf{G} + \sigma^2 E\left\{(\boldsymbol{\alpha}^2\mathbf{E})^{-1}\right\}\right]^{-1}, \tag{8}$$

where $E\{\cdot\}$ denotes statistical expectation. Note that in (8), we replaced the temporal cross-correlation matrix $\mathbf{R}$ with the estimate of the space-time cross-correlation matrix $\hat{\mathbf{G}}$ [14]. At the output of the space-time MUD, users' data estimates are then given by

$$\hat{\mathbf{b}} = \text{sgn}\left[\Re\left\{\boldsymbol{\alpha}^{\mathbf{H}}\mathbf{T}_{MMSE}\mathbf{Y}\right\}\right], \tag{9}$$

where sgn$(\cdot)$ denotes the signum function, and $\Re\{x\}$ denotes the real part of the complex value x.

IV. PERFORMANCE ON THE AWGN CHANNEL

In this Section, we first present the Gaussian approximation for the space-time MMSE-MUD [15] and then use this approximation to obtain error bounds for the coded system. We also present simulation examples to assess the accuracy of our analytical results when compared to exact system's performance.

A. RS Performance Bounds

In [15], Poor and Verdu have proved that the probability of bit error for the MMSE-MUD can be estimated using the Gaussian approximation given by,

$$P_k = Q\left(\frac{\mu}{\sqrt{1+\lambda^2}}\right), \tag{10}$$

where $Q(x)$ is the complementary Gaussian cumulative distribution function, $Q(x) = \int_x^\infty \frac{1}{\sqrt{2\pi}} e^{-y^2/2} dy$. Here, $\mu = \frac{\sqrt{E_k}(\mathbf{TR})_{kk}}{\sigma\sqrt{(\mathbf{TR}\,\mathbf{T}^H)_{kk}}}$ and $\lambda^2 = \mu^2 \sum_{j\neq k}^K \xi_j^2$ with $\xi_j = \frac{\sqrt{E_j}(\mathbf{TR})_{kj}}{\sqrt{E_k}(\mathbf{TR})_{kk}}$ known as the leakage coefficient [15]. Using an antenna array, at the receiver side, the same approximation can be made by simply replacing the cross-correlation matrix $\mathbf{R}$ with the space-time cross-correlation matrix $\mathbf{G}$.

Since an evaluation of the exact bit error rate (BER) performance of a RS decoder requires complete knowledge of the bit error location, an upper bound was introduced in [16] and used here for the space-time system. Given the Gaussian approximation in (10), such an upper bound is defined for the kth user by

$$P < \frac{2^m}{2^m - 1} \sum_{i=t+1}^{n} \binom{i+t}{n} \binom{n}{i} P_s^i (1-P_s)^{n-i}, \tag{11}$$

where $\binom{n}{i} = \frac{n!}{(n-i)!i!}$, t is the error correction capability of the code, and P_s is the symbol error rate, given at the output of the MMSE-MUD by

$$P_s = \sum_{e=1}^{\chi} \binom{\chi}{e} P_k^e (1-P_k)^{\chi-e}, \tag{12}$$

with P_k defined in (10), and χ is an integer defined by Galois field $GF(q^\chi)$ [16].

B. CC Performance Bounds

We start by defining the BER upper bounds for the hard decision (HD) Viterbi decoder, and then follow with the soft decision case.

Considering a binary symmetric channel (BSC), representing the AWGN channel plus the space-time detector, the upper bound for the probability of bit error is given by [17]

$$P_b < (1/m) \sum_{d=d_{free}}^{\infty} \beta_d P_2(d), \tag{13}$$

where the terms β_d represent the coefficients of the derivative of the CC transfer function $F(D,N)$ and $P_2(d)$ is the pairwise error probability. Using the Chernoff bound [17], the error bound in (13) can be written as

$$P_b < (1/m) \frac{\partial F(D,N)}{\partial N} \Big|_{N=1, D=2\sqrt{p(1-p)}}, \tag{14}$$

where p is the BSC probability of bit error given in (10).

Moving on to the soft decision case, and using the Gaussian approximation, it is not difficult to show that the probability of bit error for the kth user is given by

$$P_b < (1/m) e^{d_{free} E_k (TG)_{kk}^2 / 2\sigma_{kk}^2} Q\left(\frac{d_{free} E_k (TG)_{kk}^2}{\sigma_{kk}^2}\right) \times \frac{\partial F(D,N)}{\partial N} \Big|_{N=1, D=e^{-E_k (TG)_{kk}^2 / 2\sigma_{kk}^2}}, \tag{15}$$

where $\sigma_{kk}^2 = \sum_{j\neq k}^K E_j (\mathbf{TG})_{kj} + \sigma^2 (\mathbf{TGT}^H)_{kk}$ is the multiuser interference plus the Gaussian noise.

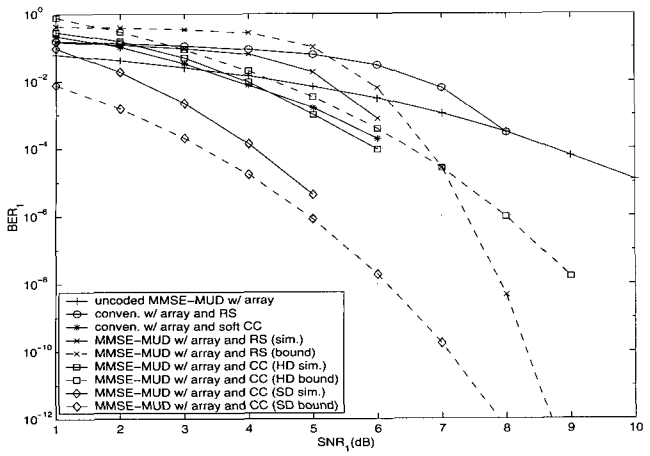

(a)

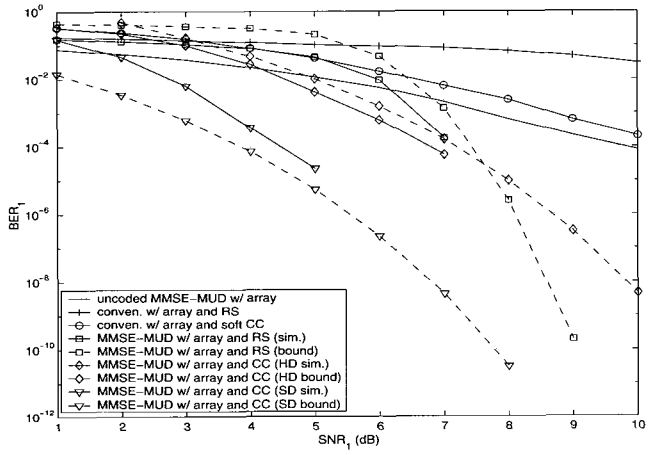

(b)

Fig. 2. Performance bounds for CC and RS coded systems with rate 1/2 over the AWGN channel: (a) $\theta_1 = 0^o$, and interfering users at $\theta = \pm 15^o, \pm 30^o, \pm 45^o$, and 60^o. (b) $\theta_1 = 0^o$, and interfering users at $\theta = \pm 5^o, \pm 20^o, \pm 35^o$, and 50^o.

C. *Simulation Results*

In what follows, we examine the performance of the coded space-time system introduced in the previous Section. A Binary -Phase shift keying (BPSK) modulation is used over the AWGN channel. The remaining system parameters are defined as follows.

- We are interested in systems with low processing gain of PG=16 for the uncoded system. Also, the use of random spreading codes is considered in our simulations.
- The RS code used is based on RS (63,m) with codeword symbols taken from the Galois field $GF(64)$.
- The convolutional code used is of rate $1/2$ and constraint length $L = 7$, or will be otherwise specified.
- The turbo code used consists of 2 identical recursive systematic convolutional (RSC) encoders with generator polynomial given in octal form by $g = \{75\}$ denoting a turbo code with two 4-state encoders. The decoder is based on the log-MAP decoding algorithm. A computer program for this algorithm is given in [18] and was tested against the standard results in [19]
- The receiver base-station is equipped with a uniform-linear array (ULA) consisting of 3 antenna elements or otherwise mentioned.
- We consider a relatively low number of users, $K = 8$, and the desired user is taken to be user #1.
- Finally, in order to produce a fair comparison between the coded system and the uncoded one (i.e. fixed channel bandwidth constraint), we compensate for the increase in the coded system's bandwidth by lowering its processing gain.

Fig. 2(a) shows the simulation results along with BER upper bounds for the space-time MMSE-MUD and using both RS and convolutional codes. Also shown are the performances for the uncoded space-time MMSE-MUD and the coded conventional detector with antenna array. In these results, users' AOA's are taken arbitrarily at $\theta_1 = 0^o$, $\theta_2 = 15^o$, $\theta_3 = -15^o$, $\theta_4 = 30^o$, $\theta_5 = -30^o$, $\theta_6 = 45^o$, $\theta_7 = -45^o$ and $\theta_8 = 60^o$. In Fig. 2, the solid line plots represent simulation results whereas the broken lines represent the coded system BER upper bounds. We first focus on the simulation results, and then follow with the performance error bounds. An inspection of the results in Fig. 2(a) reveals that, use of either the RS or the CC results in substantial BER improvements for the multiuser detector relative to the conventional matched filter detector. Specifically, the capability of CC in combating reasonable levels of multiuser interference (MI) is evident from the conventional detector curve as opposed to RS coding. Also for the space-time MUD, it is clear from extrapolating the results in Fig. 2 that the SD-CC outperforms the RS code at all practical BER levels. For instance, the former is shown to offer a coding gain of approximately 2.5 dB higher than the latter at BER of 10^{-4}. On the other hand, it appears through extrapolation that the RS code will outperform the CC at very low BER's. This phenomenon will also occur in future curves. However, for the space-time MUD examined here, this cross-over appears too small to be practical. This, in turn, contradicts with the results reported earlier for the single user AWGN channel in [1].

To examine the sensitivity of the space-time system to higher levels of multiuser interference, we consider a scenario where the AOA's are closely packed with $\theta_1 = 0^o$, $\theta_2 = 5^o$, $\theta_3 = -5^o$, $\theta_4 = 20^o$, $\theta_5 = -20^o$, $\theta_6 = 35^o$, $\theta_7 = -35^o$, and $\theta_8 = 50^o$. The results of this investigation are shown in Fig. 2(b). As noted from these results, the increased interference level results in BER degradation for the uncoded system whereas the convolutionally coded system is shown to offer 1 dB coding gain higher than the results in Fig. 2(a). Also, as expected, the performance of both the space-time matched filter and the RS coded system appear to be very sensitive to higher levels of multiuser interference.

C.1 Coded System Upper Bounds

Since it is difficult to obtain an exact expression for the CC generating function at large constraint lengths, we only consider the first five, distinct, Hamming distances and their coefficients to get the BER in (15). Also, since the main purpose of obtain-

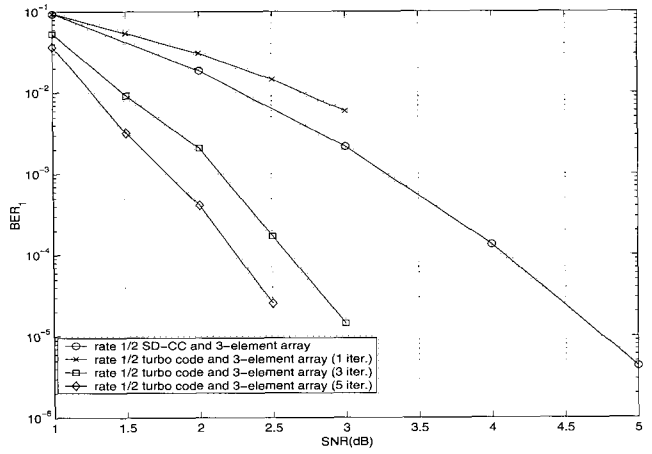

Fig. 3. Performance of punctured rate 1/2 turbo code with encoder interleaver of size 900 in space-time MMSE-MUD and $\theta_1 = 0^o$, interfering users at $\theta = \pm 15^o, \pm 30^o, \pm 45^o, 60^o$.

ing BER upper bounds is to assess the system performance at low BER levels where computer simulations become impractical and as such, the trellis paths with the least Hamming distances will constitute the major error events effecting the overall system performance.

Examining the upper bounds in Fig. 2, we find that as the SNR increases, the bounds come to an excellent agreement with the simulation results. For instance, a tolerance of only 0.5 dB is incurred at BER of 10^{-4}. It is important to note that the upper bound for the SD-CC is obtained for the infinite quantization case whereas our simulations are based on 8 levels of quantization which is usually used in practice [20]. Use of these error bounds confirms our previous conjecture that RS codes outperform SD-CC's at extremely low BER's where the cross-over BER is found to be less than 10^{-15}.

C.2 The Turbo Coded System

As an interesting comparison, we consider the application of rate 1/2 turbo codes in the space-time system. Here we use a random encoder interleaver for its large potential gain relative to block and convolutional interleavers [21], [22]. Using an interleaver of size 900 symbols, the BER performance is shown in Fig. 3 for different number of decoding iterations. For comparison reasons, we also include the performance of the SD-CC which is known to offer a complexity comparable to the turbo code used [23]. As shown in Fig. 3, the performance of the turbo coded system starts to improve at 3 and 5 decoding iterations where iterative decoding becomes more efficient. For instance, a coding gain as much as 2 dB higher than the SD-CC is seen at 5 iterations and BER of 10^{-5}.

V. PERFORMANCE ON THE RAYLEIGH FADING CHANNEL

In this section, we obtain the probability of bit error for the uncoded space-time MMSE-MUD in flat Rayleigh fading channels assuming ideal channel interleaving that produce independent fading statistics for each symbol period. In addition, analytical error bounds are obtained for the coded system. Finally, we introduce simulation examples to check the accuracy of these analytical results.

A. BER Analysis

Employing the linear MMSE-MUD, and assuming that the desired user channel coefficient is perfectly known at the receiver, the optimum decision rule for the kth user is given by

$$\hat{b}_k = \mathrm{sgn}\left[\Re\left(\left(\mathbf{T}_{mmse}\mathbf{Y}\right)_k \alpha_k^*\right)\right] = \mathrm{sgn}\left(\tilde{b}_k\right). \tag{16}$$

Now, following the formulation in [15], (16) can be written as

$$\tilde{b}_k = \sqrt{E_k}\,|\alpha_k|^2\, b_k(\mathbf{TG})_{kk} + \Re\left\{\sum_{j=1, j\neq k}^{K} \sqrt{E_j}\alpha_k^*\alpha_j(\mathbf{TG})_{kj}\, b_j\right\} + n_k, \tag{17}$$

where n_k is Gaussian random variable with mean zero and variance $\sigma^2\,|\alpha_k|^2\,(\mathbf{TGT}^H)_{kk}$.

Conditioning the probability of bit error on the channel coefficients, it is easy to show that

$$P_k(\hat{b}_k = 1 \mid \alpha_1, \cdots, \alpha_j, \cdots, \alpha_K) = \frac{1}{2^{K-1}} \sum_{b_1\in\{-1,1\}} \cdots \sum_{b_{j\neq k}\in\{-1,1\}} \cdots \sum_{b_K\in\{-1,1\}} Q\left(\frac{\sqrt{E_k}\,|\alpha_k|\,\{(\mathbf{TG})_{kk}\}}{\sigma\sqrt{\{(\mathbf{TGT}^H)_{kk}\}}} + \frac{\sum_{j\neq k}^{K}\sqrt{E_j}\, b_j \Re\{\alpha_k^*\alpha_j(\mathbf{TG})_{kj}\}}{\sigma\,|\alpha_k|\sqrt{(\mathbf{TGT}^H)_{kk}}}\right) \tag{18a}$$

$$= \frac{1}{2^{K-1}} \sum_{b_1\in\{-1,1\}} \cdots \sum_{b_{j\neq k}\in\{-1,1\}} \cdots \sum_{b_K\in\{-1,1\}} Q\left(\frac{\sqrt{E_k}\,|\alpha_k|}{\sigma}\Lambda_{kk} + \sum_{j\neq k}^{K}\frac{\sqrt{E_j}\Re\left\{\alpha_k^*\alpha_j e^{i\psi_{kj}}\right\} b_j}{\sigma\,|\alpha_k|}\,|\Lambda_{kj}|\right), \tag{18b}$$

where the parameter $\Lambda_{kj} = \frac{|(\mathbf{TG})_{kj}|e^{i\psi_{kj}}}{\sqrt{(\mathbf{TGT}^H)_{kk}}}$. We note that a Gaussian approximation on the multiuser interference does not have to be made as the Rayleigh fading assumption makes this interference Gaussian. Averaging (18b) with respect to the fading coefficients, and assuming that the transmitted bits are equiprobable, we have

$$P_{k|\alpha_k} = E\left(Q\left(\frac{\sqrt{E_k}\,|\alpha_k|}{\sigma}\Lambda_{kk} + \sum_{j\neq k}^{K}\frac{\sqrt{E_j}\Re\{\alpha_j\}}{\sigma}\,|\Lambda_{kj}|\right)\right) \tag{19}$$

In (19), we discarded the phase term $\frac{\alpha_k^* e^{i\psi_{kj}}}{|\alpha_k|}$, and b_j as they do not effect the mean and the variance of the Gaussian random

variables $\Re\{\alpha_j\}$. Also since $\Re\{\alpha_j\}$ $j = 1, \cdots \neq k, K$ represent independent Gaussian random variables, the probability of bit error conditioned on α_k is given by

$$P_{k|\alpha_k} = Q\left(\frac{\frac{\sqrt{E_k}}{\sigma}|\alpha_k|\,\Lambda_{kk}}{\sqrt{1+\sum_{j\neq k}^{K}\frac{E_j}{\sigma^2}|\Lambda_{kj}|^2}}\right). \tag{20}$$

To obtain the probability of bit error for the kth user, we average (20) over the Rayleigh distribution to give [24]

$$P_k = \int_0^\infty \alpha_k e^{-\alpha_k^2/2} Q\left(\frac{\frac{\sqrt{E_k}}{\sigma}|\alpha_k|\,\Lambda_{kk}}{\sqrt{1+\sum_{j\neq k}^{K}\frac{E_j}{\sigma^2}|\Lambda_{kj}|^2}}\right) d\alpha_k$$

$$= \frac{1}{2}\left(1 - \frac{\sqrt{E_k}\Lambda_{kk}}{\sqrt{\sigma^2+\sum_{j=k}^{K}E_j|\Lambda_{kj}|^2}}\right). \tag{21}$$

B. RS and CC Hard Decision Upper Bounds

Having obtained the BER for the space-time MMSE-MUD in fading channels, one can define BER upper bounds for the hard decision decoders using (11), (12), (21), and by assuming a BSC consisting of the fading channel plus the multiuser detector.

C. SD-CC Upper Bounds

Considering a window of d transmitted bits, the conditional pairwise probability of error for user k is given by

$$P(d)_{\alpha_{k,1},\cdots,\alpha_{k,d}} = P\left\{\sum_{n=1}^{d}\hat{b}_{k,n} \geq 0\right\}, \tag{22}$$

where the summation in (22) is taken over the incorrect path of d bits assuming the all zero path has been transmitted. Now, the data estimate in (16) can be written for the nth transmitted bit as

$$\hat{b}_{k,n} = \sqrt{E_k}\,|\alpha_{k,n}|^2\, b_{k,n}(\mathbf{TG})_{kk} + |\alpha_{k,n}|\sum_{j\neq k}^{K}\Re\left\{\sqrt{E_j}e^{-i\phi_{k,n}}\alpha_{j,n}(\mathbf{TG})_{kj}\,b_{j,n}\right\} + n_{k,n}, \tag{23}$$

and the probability of error in (22) is then simply given by

$$P(d)_{\alpha_{k,1},\cdots,\alpha_{k,d}} = Q\left(\frac{\mu_t}{\sigma_t}\right), \tag{24}$$

where

$$\mu_t = \sqrt{E_k}\mid \mathbf{TG}\mid_{kk}\sum_{n=1}^{d}|\alpha_{k,n}|^2, \tag{25}$$

and

$$\sigma_t^2 = \sigma^2(\mathbf{TGT}^H)_{kk}\sum_{n=1}^{d}|\alpha_{k,n}|^2 + \sum_{n=1}^{d}\sum_{j\neq k}^{K}E_j\,|\alpha_{k,n}|^2 \mid \mathbf{TG}\mid_{kj}^2. \tag{26}$$

Note that equation (26) follows from the real part of the multiuser interference term $|\alpha_{k,n}|\sum_{j\neq k}^{K}\Re\{\sqrt{E_j}e^{-i\theta_{k,n}}\alpha_{j,n}$ $(\mathbf{TG})_{kj}\,b_{j,n}\}$ being Gaussian random variable with zero mean and variance $\sum_{n=1}^{d}\sum_{j\neq k}^{K}E_j\,|\alpha_{k,n}|^2 \mid \mathbf{TG}\mid_{kj}^2$ where we assumed that the fading coefficients are independent among users and from one bit-to-another. Substitution of (25) and (26) in (24) yields

$$P(d)_{\alpha_{k,1},\cdots,\alpha_{k,d}} = Q\left(\sqrt{\frac{E_k\mid \mathbf{TG}\mid_{kk}^2\sum_{n=1}^{d}|\alpha_{k,n}|^2}{\sigma^2(\mathbf{TGT}^H)_{kk}+\sum_{j\neq k}^{K}E_j\mid \mathbf{TG}\mid_{kj}^2}}\right), \tag{27}$$

which represents a Chi-square distribution with $2d$ degrees of freedom for the $|\alpha_{k,n}|^2$ terms. Averaging of (27) over the Chi-square distribution [24], gives the probability of error as

$$P(d) = [\frac{1}{2}(1-\gamma)]^d\sum_{n=0}^{d-1}\binom{d-1+n}{n}[\frac{1}{2}(1+\gamma)]^n, \tag{28}$$

where

$$\gamma = \sqrt{\frac{SINR_{av}}{SINR_{av}+1}},$$

and

$$SINR_{av} = \frac{(E_k/2\sigma^2)\mid \mathbf{TG}\mid_{kk}^2 E(|\alpha_{k,n}|^2)}{(\mathbf{TGT}^H)_{kk}+\sum_{j\neq k}^{K}(E_j/\sigma^2)\mid \mathbf{TG}\mid_{kj}^2}$$

is the average signal-to-noise plus interference ratio per coded bit. Having obtained the pairwise probability of error, we can find the probability of bit error upper bound in (13). Note that the probability of bit error in (28) is similar to the one obtained for the conventional maximal-ratio combiner (MRC) with a diversity order equal to d. This is not surprising since channel coding is some form of time diversity with diversity order equal to the minimum Hamming distance of the channel code being used.

D. Simulation Results

In the following simulation results, we consider a flat fast-fading channel in which the channel variations are considered constant over one symbol interval.

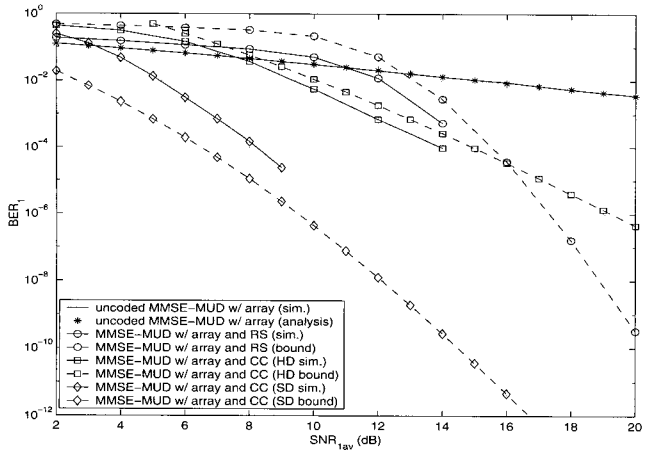

Fig. 4. Performance of RS and CC coded systems over a Rayleigh fading channel and code rate 1/2, $\theta_1 = 0^o$, and interfering users at $\theta = \pm 5^o, \pm 20^o, \pm 35^o$, and 50^o.

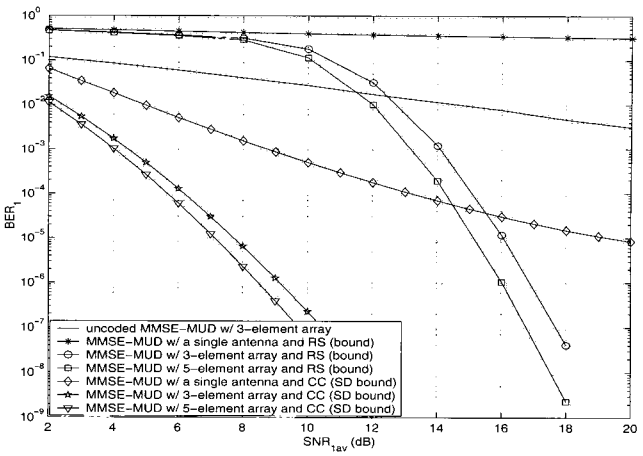

Fig. 5. Effect of increasing the number of antennas on the BER performance on flat fading channel and large angular distributions and code rate 1/2.

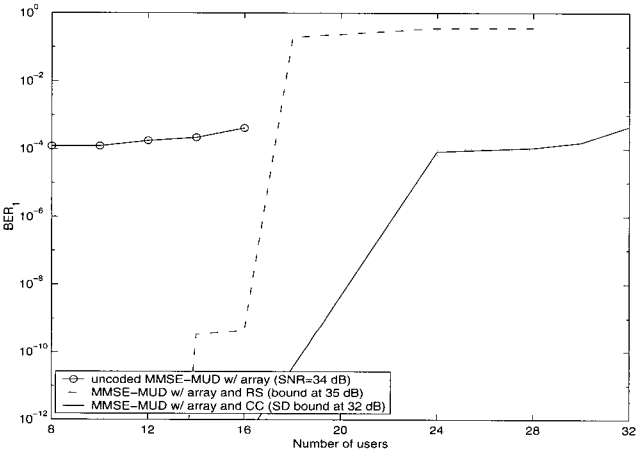

Fig. 6. Capacity investigation of the coded space-time MMSE-MUD using BER upper bounds with code rate 1/2. $\theta_1 = 0^o$, and interfering users at $\theta = \pm 5^o, \pm 20^o, \pm 35^o$, and 50^o. All extra users are at $\theta_k = 0^o$.

D.1 BER Performance

Fig. 4 shows the performance plots for both RS and CC using the space-time MMSE-MUD. The performance of the uncoded MUD is also shown along with our analytical results given in the previous section. Since the BER performance of the conventional detector is known to be quite poor for the fading channel, in what follows, we only focus on the performance of the space-time multiuser detector. As the results in Fig. 4 reveal, the use of antenna arrays plus MUD is shown to improve the interference cancellation process whereas channel coding overcomes the degradation caused by the fading process. With regard to the uncoded system, Fig. 4 shows the complete agreement of our analytical results with the exact system's performance. Also, as was shown earlier for the AWGN channel, the SD-CC offers a better performance than the RS code at all practical BER levels. It is found that the cross-over BER between RS and SD-CC is larger than the AWGN channel, and is inversely proportional to the level of multiuser interference introduced. This fact will be shortly justified when we discuss BER upper bounds.

Let us now examine the coded system error bounds derived in the previous section. Examining the results in Fig. 4, one can see that such error bounds become more tight with a small tolerance for BER's lower than 10^{-4}. For example, at a BER of 10^{-4} both HD-CC and RS error bounds show a loss of one magnitude away from the exact results. On the other hand, the SD-CC error bound is about 1.5 dB away from the exact performance. Furthermore, the cross-over BER between RS and SD-CC is shown here to be well below 10^{-12} agreeing with our previous discussions.

D.2 Effect of Varying the Number of Antennas

In Fig. 5, the BER performance as a function of the number of antenna elements is shown. As a bench mark, we also show the performance of the uncoded MMSE-MUD with 3-element array. The single antenna case is significant here since it represents the ability of channel coding in combating cochannel interference when no interference cancellation is used besides the MUD. As noted from these results, the convolutionally coded system (with no spatial interference cancellation) is able to perform better than the uncoded system with 3-antenna array. This is important since conserving antenna array processing is of practical interest. Also, it is observed that increasing the number of antennas above 3 has a little impact on the BER performance.

D.3 Capacity Improvements

As was discussed earlier, error bounds can be of a great importance especially when the system is heavily loaded (i.e., $K > 8$ users). Here, we use the analytical results obtained earlier to estimate the gain achieved using error control coding in view of user-capacity. That is, we translate the achieved coding gain into additional number of users under fixed BER and SNR constraints. Fig. 6 describes the results of such an investigation. The BER performance versus the number of users is shown in this figure for the uncoded system and for both the RS and SD-CC systems. The angular distribution for the arriving signals is taken at $\theta_1 = 0^o, \theta = \pm 5^o, \pm 20^o, \pm 35^o, 50^o$, and any additional user is assumed to arrive at the same AOA as the desired user (i.e., $\theta_{k>8} = 0^o$). Also, for reasons of discussion, the

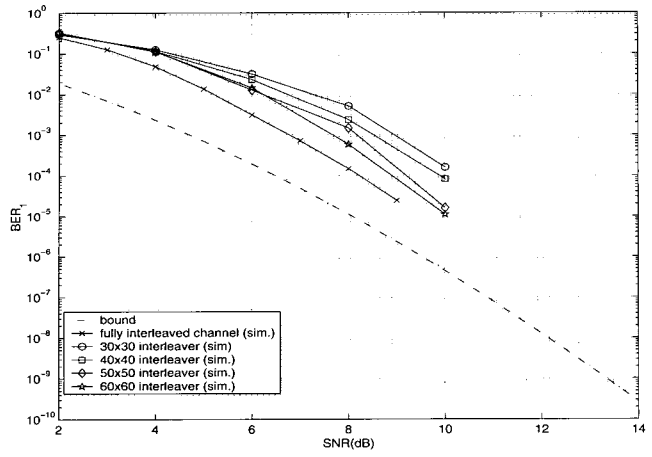

Fig. 7. BER performance in a flat Rayleigh fading channel with normalized fade f_d=0.01, N=3, rate 1/2 SD-CC and channel interleaving.

SNR is fixed to 34 dB. Note that the tolerance in the BER upper bounds from the actual simulations is compensated to allow for a realistic investigation. As shown in Fig. 6, the performance of the RS coded system exhibits an abrupt drop which is evident from the slope of the curve at a system load of 16 users. On the other hand, the CC system can handle up-to 28 users relative to the uncoded 8-user system at a prescribed BER of 10^{-4}. This, in turn, gives an increase in system's user-capacity of approximately 250% relative to the uncoded system and 150% relative to the RS coded system. Note that the rapid change in the slope at the capacity point is due to the loss in coding gain, which has no impact on the capacity gain. We have also observed that larger capacity gains can be easily achieved at BER's lower than 10^{-4}.

D.4 Channel Interleaving

Thus far, we have only considered a fully interleaved channel with independent fading statistics. Let us now examine the effect of including a more realistic channel model with some memory. Since it is difficult to obtain analytical results for a correlated fading channel, we will only rely on simulation results and then check these results against ideal cases. Again, the system is shown in Fig. 1 with a practical interleaver/deinterleaver pair. Depending on the size of the interleaver, successive source symbols experience reduction in the correlation among their fades during transmission. There are several types of channel interleavers that have been introduced in the literature [16]. In our work, we consider a simple block interleaver of size yz where y and z represent the number of rows known as the interleaving depth, and the number of columns known as the interleaving span, respectively. Note that the statistical behavior of the interleaving process depends mainly on the choice of the interleaving parameters y and z which in turn depend on the channel fade variations and the decoding depth. In characterizing the time variations of the fading channel, we choose a Doppler rate, normalized to the bit rate, f_d equal to 0.01. This large normalized Doppler rate signifies fast time variations in the fading process relative to the transmission bit rate. Here, the fast fading process was generated by passing a white Gaussian noise through

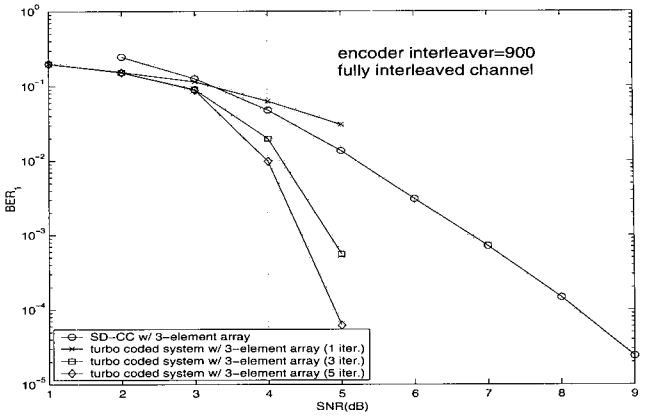

(a)

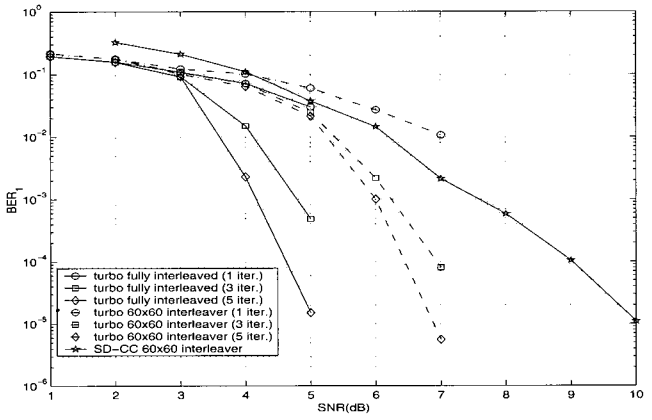

(b)

Fig. 8. Performance of punctured rate 1/2 turbo code with random encoder interleaver, $\theta_1 = 0^o$, and interfering users at $\theta = \pm 5^o$, $\pm 20^o$, $\pm 35^o$, and 50^o: (a) a fully interleaved fading channel, (b) with channel interleaving.

a third order low pass filter (i.e., 3rd order Butterworth filter) [25]. Furthermore, for interleaving to be effective, we set the interleaving span to be larger than 30 symbols (i.e., the decoding depth $L_d = 30$). Also, since it is impractical to choose the interleaving depth larger than the maximum fading depth, we consider a block interleaver of size yz where $z = y$ and greater than the decoder depth.

Fig. 7 shows the performance results, for the system described above, with different interleaving degrees along with the BER upper bounds for the ideal interleaving case. As seen, a loss of less than an order of 1 dB is incurred due to practical interleaving. For example, only 0.6 dB coding loss results for a relatively small interleaver of size 3600 symbols for the correlated fading channel relative to the ideal interleaving case.

D.5 Turbo Codes on Fully Interleaved Channels

In Fig. 8(a), we simulate the turbo coded system over a fully interleaved fading channel using an encoder interleaver of size 900 symbols. As shown from this figure, turbo codes perform

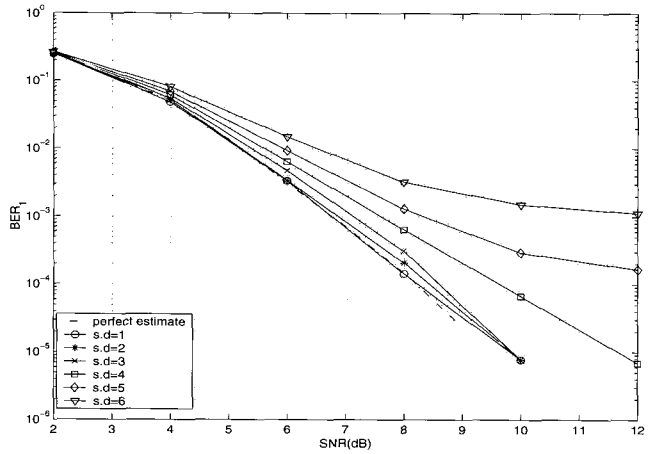

Fig. 9. Convolutionally coded system with sensitivity to AOA estimation errors. $\theta_1 = 0^o$, and interfering users at $\theta = \pm 5^o, \pm 20^o, \pm 35^o$, and 50^o.

better than SD-CC with a relative coding gain of approximately 3 dB at BER of 10^{-5} and using 5 decoding iterations. Also, as in the AWGN channel, the error flooring effect exhibited by the turbo code at 5 iterations is evident from Fig. 8(a).

D.6 Turbo Codes with Non-ideal Channel Interleaving

Here, we examine the performance of turbo codes in the space-time system and considering a correlated fading channel. It will be seen that the presence of fading correlation poses a major problem to the turbo coded system. The BER performance is shown in Fig. 8(b) with a fixed random encoder interleaver of size 1800 symbols and a block channel interleaver of size 60×60 symbols. In this case, the use of practical channel interleaving results in a coding gain loss of 2 dB from the fully interleaved channel at 3 and 5 decoding iterations. This loss is shown to be much higher than the one seen earlier for SD-CC (Fig. 7). Note that the relative coding gain between the turbo coded system and the SD-CC one is shown to be in the range of 2.5 dB, a coding gain loss of 0.5 from the fully interleaved case. On the other hand, in an adaptive MMSE receiver, we found that the relative coding gain between turbo codes and SD-CC's to be smaller than the gain obtained for the multiuser-type receiver [12].

D.7 Sensitivity to AOA Estimation Errors

In this section, we study the sensitivity of the space-time system to estimation errors in the antenna array steering vector. In this discussion, we only consider the effect of estimation errors on the convolutionally coded system. In that, we choose to model the AOA estimation error as an additive Gaussian distributed random variable with standard deviation (s.d) equal σ_θ. In this case, the receiver estimate is given by

$$\hat{\theta} = \theta + n_\theta, \tag{29}$$

where θ is the correct AOA and n_θ is the Gaussian estimation error with zero mean and variance ${\sigma_\theta}^2$.

In Fig. 9, we examine the performance of the convolutionally coded system with AOA estimation errors. As shown, the performance starts to significantly degrade at $\sigma_\theta = 4$. For instance, a SNR loss of approximately 1.5 dB from the ideal case is seen for a prescribed BER of 10^{-4}. As the estimation error increases beyond $\sigma_\theta = 4$, the system starts to show an error floor at higher BER levels. This is expected since the antenna array in this case enhances the cochannel interference instead of cancelling it. This, in turn, results in a performance degradation of the space-time multiuser detector and hence an ineffective decoding operation.

VI. CONCLUSIONS

In this paper, we considered the application of CC, RS and turbo codes in DS-CDMA systems that employ space-time MMSE-MUD. Initially, we introduced the space-time MMSE-MUD using these coding schemes in AWGN channels. Our simulation results demonstrated substantial BER improvements relative to the coded space-time conventional detector. The Gaussian approximation for the error analysis in AWGN channels was used to obtain error bounds for both the RS and the convolutionally coded systems. We found that, the use of space-time MUD and SD-CC can offer up-to 2.5 dB coding gain relative to RS coding. Also, the superiority of turbo codes in terms of their large coding gains relative to SD-CC was shown. For the flat fading channel, we proved that the two forms of diversity, space and time diversity, significantly enhance the system's BER. Our results show a coding gain of at least 6 dB using SD-CC relative to the RS coded system. We introduced an accurate closed form expression for the uncoded system BER. Upper bounds for the coded system were obtained and shown to be tight. A user-capacity investigation was performed where it was shown that SD-CC can offer capacity gains of approximately 250% relative to the uncoded system, and 150% relative to the RS coded system. In a correlated fading channel, where practical channel interleaving is used, we observed a small SNR loss relative to a channel with no memory. In a comparison between turbo and SD-CC, it has been shown that the former offers a superior performance than the latter with a coding gain of 2.5 dB. We examined the sensitivity of the coded system to AOA estimation errors where it was shown that the system can be quite tolerable for relatively large estimation errors.

APPENDIX

In (6), the following matrices were used and taken from [14] (it follows the notation in [3]):

$$\mathbf{Y} = \begin{bmatrix} y_1 & \cdots & y_k & \cdots & y_K \end{bmatrix}^T, \tag{30}$$

$$\hat{\mathbf{G}} = \begin{bmatrix} \hat{\mathbf{u}}_1^H \mathbf{u}_1 \rho_{1,1} & \cdots & \hat{\mathbf{u}}_1^H \mathbf{u}_k \rho_{1,k} & \cdots & \hat{\mathbf{u}}_1^H \mathbf{u}_K \rho_{1,K} \\ \hat{\mathbf{u}}_2^H \mathbf{u}_1 \rho_{2,1} & \cdots & \hat{\mathbf{u}}_2^H \mathbf{u}_k \rho_{2,k} & \cdots & \hat{\mathbf{u}}_2^H \mathbf{u}_K \rho_{2,K} \\ \cdots & \cdots & \cdots & \cdots & \cdots \\ \cdots & \cdots & \cdots & \cdots & \cdots \\ \hat{\mathbf{u}}_K^H \mathbf{u}_1 \rho_{K,1} & v & \hat{\mathbf{u}}_K^H \mathbf{u}_k \rho_{K,k} & \cdots & \hat{\mathbf{u}}_K^H \mathbf{u}_K \rho_{K,K} \end{bmatrix}, \tag{31}$$

$$\mathbf{U} = \left[\begin{array}{ccccc} \mathbf{u}_1 & \cdot & \mathbf{u}_k & \cdot & \mathbf{u}_K \end{array} \right]^T, \tag{32}$$

$$\sqrt{\mathbf{E}} = \mathrm{diag}\left[\begin{array}{ccccccc} \sqrt{E_1} & \cdots & \sqrt{E_k} & \cdots & \sqrt{E_K} \end{array} \right], \tag{33}$$

and

$$\boldsymbol{\alpha} = \mathrm{diag}\left[\begin{array}{ccccc} \alpha_1 & \cdots & \alpha_k & \cdots & \alpha_K \end{array} \right], \tag{34}$$

$$\mathbf{N} = \left[\begin{array}{ccccc} \gamma_1 & \cdots & \gamma_k & \cdots & \gamma_K \end{array} \right]^T. \tag{35}$$

The cross-correlation, $\rho_{i,j}$, is defined in (4).

ACKNOWLEDGMENT

The authors would like to thank the anonymous reviewers for their helpful comments and suggestions that helped to improve the presentation of this manuscript.

REFERENCES

[1] S. Wicker, *Error Control Systems for Digital Communication and Storage*, Prentice Hall 1995.

[2] Y. Yeh and D. Reudink, "Efficient spectrum utilization for mobile radio systems using space diversity", *IEEE Trans. Commun.* vol.30, pp447–455, Mar. 1982

[3] S. Miller and S. Schwartz, "Integrated spatial-temporal detectors for asynchronous Gaussian multiple-access channels," *IEEE Trans. Commun.*, vol. 47, no. 9, pp. 2356–2374, Sept. 1999.

[4] X. Wang and H. V. Poor, "Space-time multiuser detection in multipath CDMA channels," *IEEE Trans. Signal. Processing*, vol. 47, no. 9, pp. 2356–2374, Sept. 1999.

[5] P. Frenger, P. Orten and T. Ottosson, "Code-spread CDMA using maximum free distance low-rate convolutional codes," *IEEE Trans. Commun.*, vol. 48, no. 1, pp. 135–144, Jan. 2000.

[6] Y. Chen, K. Letaief, and J. Chuang, "Soft-output equalization and TCM for wireless personal communication systems," *IEEE J. Select. Areas Commun.*, vol. 45, pp. 1161–1172, May 1997.

[7] V. Kuhn, "Evaluating the performance of turbo codes and turbo-coded modulation in a DS-CDMA environment," *IEEE J. Select. Areas Commun.*, vol. 17, pp. 2138–2147, Dec. 1999.

[8] Y. Wong and K. Lataief, "Concatenated coding for DS/CDMA transmission in wireless communications," *IEEE Trans. Commun.*, vol. 48, no. 12, pp. 1965–1969, Dec. 2000.

[9] S. Kim, B. Yi, and R. Pickholtz, "Asymptotic performance of ML sequence estimator using an array of antennas for coded synchronous multiuser DS-CDMA systems," *J. Commun. Networks*, vol. 1, no. 3, pp. 182–188, Sept. 1996.

[10] M. Reed and P. Alexander, "Iterative multiuser detection using antenna arrays and FEC on multipath channels", *IEEE J. Select. Areas Commun.*, vol. 17, no. 12, pp. 2082–2089, Dec. 1999.

[11] T. Giallorenzi and S. Wilson, "Suboptimum multiuser receivers for convolutionally coded asynchronous DS-CDMA systems," *IEEE Trans. Commun.*, vol. 44, no. 9, pp. 1183–1196, Sept. 1996.

[12] W. Hamouda, *Performance Analysis of Space-Time Multiuser Detection with Error Correction Coding in CDMA Communication Systems*, Ph.D thesis, Queen's University, Kingston, Ontario, Canada, Apr. 2002.

[13] S. Uppala and J. Sahr, "Computing probability of errors of linear multiuser detectors in white Gaussian noise and Rayleigh fading channels," in *Proc. ICC'98.*

[14] W. Hamouda and P. McLane, "Performance analysis of Space-time MMSE detection in synchronous multiuser DS-CDMA," in *Proc. ISSSTA'00.*

[15] H. V. Poor and S. Verdu, "Probability of error in MMSE multiuser detection," *IEEE Trans. Inform. Theory*, vol. 43, no. 3, pp. 858–871, May 1997.

[16] G. Clark and J. Cain, *Error-Correcting Coding for Digital Communications*. Plenum Press, New York, 1981.

[17] A. Viterbi and J. Omura, *Principles of Digital Communication and Coding*, McGraw-Hill Publishing, 1979.

[18] Y. Wu, *http://www.ee.vt.edu/ yufei/turbo.html*, June 1999.

[19] C. Berrou and A. Glavieux, "Near Shannon limit error-correction coding and decoding: Turbo codes," in *Proc. ICC'93.*

[20] J. Heller and I. Jacobs, "Viterbi decoding for satellite and space communication," *IEEE Trans. Commun.*, vol. 44, no. 5, pp. 835–848, Oct. 1971.

[21] S. Benedetto and G. Montorsi, "Design of parallel concatenated convolutional codes," *IEEE Trans. Commun.*, vol. 44, no. 5, pp. 591–600, May 1996.

[22] P. Robertson, E. Villebrun, and P. Hoeher, "A comparison of optimal and suboptimal MAP decoding algorithms in the log domain," in *Proc. ICC'95.*

[23] L. Hanzo, T.H. Liew, and B.L. Yeap, *Turbo Coding, Turbo Equalisation and Space-Time Coding for Transmission over Fading Channel*, John Wiley & Sons, Inc., U.K, 2002.

[24] J. Proakis, *Digital Communications*, McGraw-Hill Publishing, 1995.

[25] A. Barbosa and S. Miller, "Adaptive detection of DS/CDMA signals in fading channels", *IEEE Trans. Commun.*, vol. 46, no. 1, pp. 115–124, Jan. 1998.

Walaa Hamouda received his B.Sc. degree in 1992 in Electrical Engineering from Ain Shams University, Cairo, Egypt, and his M.Sc. and Ph.D. degrees from Queen's University, Kingston, Ontario, Canada, in 1998 and 2002, respectively, all in Electrical Engineering. During his graduate studies, he was awarded the Ontario Graduate Scholarships (OGS) and Queen's Graduate Fellowship. From 1992 to 1993, he served in the Egyptian military in the Department of Telecommunications for the Ministry of Defence. From 1994 to 1995, he joined Siemens, Cairo, Egypt, in the Telecommunications Division, where he focused on the design of telecommunication cables and fiber optic transmission systems. Since July 2002, he has been appointed as an Assistant Professor with the Department of Electrical and Computer Engineering, Concordia University, Montreal, Quebec, Canada. His current research interests are in wireless and mobile communications, smart antenna techniques, channel coding, and space-time coding.

Peter J. McLane was born in Vancouver, BC, Canada, on July 6, 1941. He received the B.A.Sc. degree from the University of British Columbia, Vancouver, in 1965, the M.S.E.E. degree from the University of Pennsylvania, Philadelphia, in 1966, and the Ph.D. degree from the University of Toronto, Toronto, Ont., Canada, in 1969. From 1966 to 1967, he was a Junior Research Officer with the National Research Council, Ottawa, Ontario, Canada. He joined the Department of Electrical and Computer Engineering, Queen=s University, Kingston, Ontario, Canada, in 1969 as an Assistant Professor, and since 1977 he has held the rank of Professor. His research interests are in modulation, coding and signal processing for digital communication systems. He is a former research Trust Leader in Mobile and Satellite Systems for the Telecommunications Research Institute of Ontario (TRIO) and formerly a Major Project Leader in Mobile and Personal Communications for the Canadian Institute of Telecommunications Research (CITR). He is a joint author of Introduction to Trellis-Coded Modulation with Applications (Macmillan, 1991).Dr. McLane is an IEEE Fellow and former chair of the IEEE Communications Society Communication Theory Committee. He is a former Associate Editor for the IEEE COMMUNICATIONS MAGAZINE and a former Editor of the IEEE TRANSACTIONS ON COMMUNICATIONS. In addition, he was co-editor of single issues of the IEEE JOURNAL ON SELECTED AREAS IN COMMUNICATIONS and the IEEE COMMUNICATIONS MAGAZINE. He also served as Chairman of the IEEE ComSoc Mini-conference on Communication Theory at Globecom, 1993. He is also a member of the Association of Professional Engineers of Ontario and is listed in American Men and Women in Science. In 1994, he was a joint recipient of the Stentor Telecommunications Research Award. In his graduate studies he held a Ford Foundation Fellowship at the University of Pennsylvania and a National Research Council of Canada Scholarship at the University of Toronto.